Vortex Interaction Simulation

Aaron Wienkers

Abstract

I present the results of two-dimensional inviscid vortex interaction simulations for various aircraft and vortex configurations. The formation of fully developed trailing wake turbulence vortices under optimum elliptical wing loading conditions was also simulated. One novel configuration to help mitigate wake turbulence was proposed which uses wing tip flaps to instigate pairs of symmetric counter-rotating vortices, which behave much less violently compared to the co-rotating vortices, as measured by a reduction in effective vortex strength, $\Gamma_{\text{effective}}$, by a factor of 4.5.

1 Problem

Vortices frequent themselves trailing behind large, heavy, and slow aircraft in the form of wake turbulence. These vortices pose unseen dangers to smaller aircraft at worst, and take credit for airport departure delays at best. The ten largest Class B airports reported being limited by the Federal Aviation Administration requirement to leave a two minute dissipation period between departing aircraft. Aircraft design has only begun to take this detriment into consideration and attempt to mitigate these wake vortices. One such configuration utilizing wing tip flaps produces symmetric counter-rotating vortex pairs which prove to be unstable and annihilate quickly in 3-D simulations when compared to co-rotating vortices seen behind all aircraft in the commercial fleet today. This instability is not able to be simulated in two dimensions, however, so wake magnitude would have to be based on variables accessible in a seemingly stable 2-D simulation, such as an effective vortex strength ratio, $\Gamma_{\text{effective}}/\bar{\Gamma}$.

2 Formulation

Various point vortex situations were analyzed using a MATLAB simulation based on the simultaneous solution of $2n+1$ ordinary differential equations, where n is the number of vortices in the system. Following Helmholtz' Law, a vortex will follow the fluid flow; thus, the induced velocity field must be defined. The induced velocity at $\mathbf{r}$ from a point vortex of strength Γ_j located at $\mathbf{r}_j$ is

$$\mathbf{u}(\mathbf{r}) = \frac{\Gamma_j}{2\pi(\mathbf{r}-\mathbf{r}_j)^2}\,\mathbf{k}\times(\mathbf{r}-\mathbf{r}_j)$$

Put into a 2-D cartesian coordinate system, where $\mathbf{r}_j =< x_j,\, y_j >$ this expression becomes

$$\mathbf{u}_j(\mathbf{r}) = \frac{\Gamma_j}{2\pi[(x-x_j)^2+(y-y_j)^2]}\,[-(y-y_j)\cdot\hat{\imath}+(x-x_j)\cdot\hat{\jmath}]$$

Summing up the effect of each vortex explicitly at vortex i, the total induced fluid velocity at $\mathbf{r}_i$ is

$$\mathbf{U}_i = \sum_{j=1,\, j\neq i}^{n} \frac{\Gamma_j}{2\pi[(x_i-x_j)^2+(y_i-y_j)^2]}\,[-(y_i-y_j)\cdot\hat{\imath}+(x_i-x_j)\cdot\hat{\jmath}]$$

which becomes the discrete set of $2n$ ordinary differential equations in the $\hat{\imath}$ and $\hat{\jmath}$ directions for $1 \le i \le n$

$$\frac{d\mathbf{r}_i}{dt} = \mathbf{U}_i(\mathbf{r}_i - \mathbf{r}_j)$$

The additional differential equation in the simultaneous setup is a $\Gamma = 0$ placeholder with initial conditions at the origin equal to naught. This "vortex" was used to determine the fluid velocity at $(\bar{x}, \bar{y})$, the mean position of each point vortex, as a function of time. The effect of the wing tip flaps was quantified as the magnitude of the central vortex-induced fluid downwash. To remove dependence on r, γ, and Γ, a ratio $\frac{\Gamma_{\text{effective}}}{\bar{\Gamma}}$ was termed, where $\Gamma_{\text{effective}}$ is the strength of vortex required to induce a fluid velocity from distance $\bar{r}$ away and $\bar{\Gamma}$ is the averaged vortex strength, $\frac{\gamma * \Gamma + \Gamma}{2}$. This ratio does not imply anything about the instability of a configuration, however, since the simulations are limited to 2 Dimensions.

3 Implementation

A MATLAB adaptive ordinary differential equation solver algorithm utilizing an explicit Runge-Kutta (4, 5) of Dormand-Prince pair was employed to simultaneously solve for the position of each vortex as a function of time. After removing and ordering the placeholder solutions, the remaining coordinate points were plotted, marking a dot at each time step of $\tau = 2$ s to improve vortex evolution visualization.

Throughout simulations, the strength of each vortex was arbitrarily assumed $\Gamma = 2\pi$ for convenience. Additionally, the wingspan of the aircraft was assumed $b = 4$ to mitigate medium order method error in solving the system and so that realistic time scales could be used.

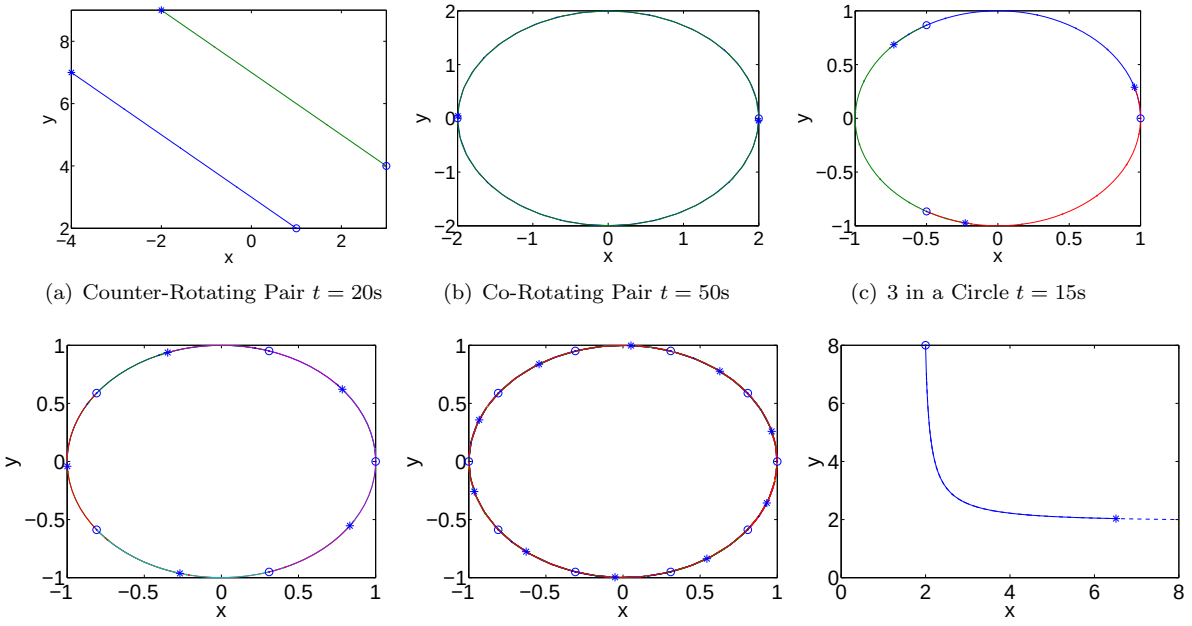

(a) Counter-Rotating Pair $t = 20$s (b) Co-Rotating Pair $t = 50$s (c) 3 in a Circle $t = 15$s

(d) 5 in a Circle $t = 15$s (e) 10 in a Circle $t = 10$s (f) Vortex on Corner and $r\sin 2\theta = cons$

Figure 1: Test cases used to verify 2-D simulation code.

The MATLAB program was confirmed by comparing basic test cases (Figure 1.a through 1.f) against knowledge of their definite trajectories. A simple pair of vortices, $\Gamma_1 = -\Gamma_2$ (Figure 1.a), was confirmed to move at constant velocity and in a straight line. Subsequently, when $\Gamma_1 = \Gamma_2$ (Figure 1.b) in that pair, it is observed that the vortices move around their centroid at constant angular velocity. When additional vortices were placed equidistant in a circle, they similarly were observed to orbit their centroid as expected in Figures 1.2-1.e (for $n = 3, 5, 10$). As a final test case, the interaction of a single vortex approaching a corner was confirmed to traverse a path $r\sin 2\theta = constant$. Three image vortices were used—one in each quadrant—to preserve the

impermeability boundary conditions at $y = x = 0$. The plot was then cropped to the wall and overlaid with the graph of $r\sin 2\theta = constant$.

The evolution of various systems of vortices of interest were calculated and then plotted given the system initial conditions, $(x, y, \Gamma)_i$ for the following aircraft configurations with $\gamma = 0.2,\ 0.4,\ \&\ 0.6$:

1. Symmetric co-rotating vortex pairs simulating vortex wake with traditional inboard flaps:

$$\big[(-b/2, 0, -\Gamma), (-b/4, 0, -\gamma\Gamma), (b/4, 0, +\gamma\Gamma), (b/2, 0, +\Gamma)\big]$$

2. Symmetric counter-rotating vortex pairs simulating vortex wake with wing tip flaps:

$$\big[(-b/2, 0, -\Gamma), (-b/4, 0, +\gamma\Gamma), (b/4, 0, -\gamma\Gamma), (b/2, 0, +\Gamma)\big]$$

3. Symmetric co-rotating vortex pairs interacting with the ground at $y = 0$:

$$\big[(-b/2, b/2, -\Gamma), (-b/4, b/2, -\gamma\Gamma), (b/4, b/2, +\gamma\Gamma), (b/2, b/2, +\Gamma)\big]$$

   with four image vortices to maintain the no penetration boundary condition[1] at $y = 0$:

$$\big[(-b/2, -b/2, +\Gamma), (-b/4, -b/2, +\gamma\Gamma), (b/4, -b/2, -\gamma\Gamma), (b/2, -b/2, -\Gamma)\big]$$

4. Vortex sheet roll up provided ideal elliptical loading, simulated as the vortex strength matching the derivative of the loading distribution (Figure 5.d):

$$(y_i,\ \Gamma_i) = \Big(\frac{i + 1/2}{N}, \frac{(2i+1)/N}{\sqrt{1 - (i + 1/2)^2/N^2}}\Big) \qquad i = -N, \ldots, 0, \ldots, N - 1$$

   for $N = 10,\ 20,\ \&\ 50$ vortices. For $N = 50$, a $(2, 3)$ Bogacki and Shrampine solving scheme was adopted to boost function efficiency and decrease time complexity.

4 Results

In the first set of simulations involving co-rotating pairs (Figure 2), it was noted that each vortex in the pair traverse the pair centroid in the same direction. As the vortices in a particular pair become closer in strength, it is observed that they orbit more tightly and faster. These pairs also descend at a higher rate, since the induced velocity at the opposing pair due to the inner vortex increases as $v_{induced} \propto \gamma$.

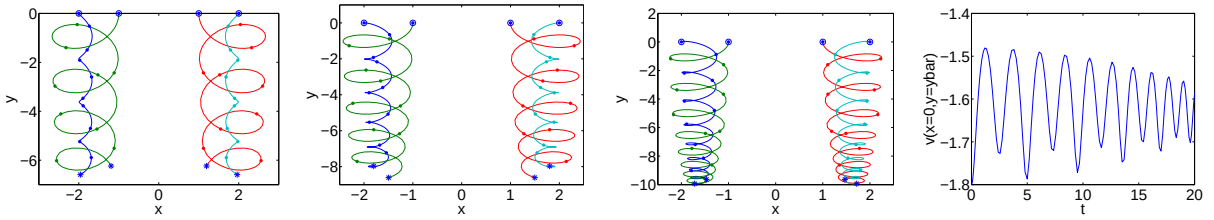

(a) $\gamma = 0.2 \quad t = 20$ s (b) $\gamma = 0.4 \quad t = 20$ s (c) $\gamma = 0.6 \quad t = 20$ s (d) Velocity at $(\bar{x}, \bar{y}) \quad \gamma = 0.4$

Figure 2: Symmetric Co-Rotating Vortex Pairs

Compared to the co-rotating pairs, counter-rotating pairs (Figure 3) have an orbital period that is much slower (almost 7 times slower for $\gamma = 0.6$). It also follows then that their mutual orbit radius increases with γ, with the limiting case at $\gamma = 1$ resulting in parallel vortex pairs[2] (Figure 1.a). The vortex pairs also sink at a decreased rate as compared to co-rotating pairs, which is attributed to the induced velocity decreasing with increasing γ.

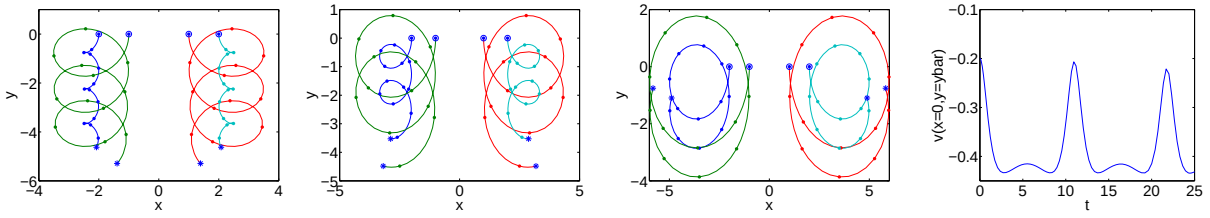

(a) $\gamma = 0.2 \quad t = 25$ s (b) $\gamma = 0.4 \quad t = 25$ s (c) $\gamma = 0.6 \quad t = 25$ s (d) Velocity at $(\bar{x}, \bar{y}) \quad \gamma = 0.4$

Figure 3: Symmetric Counter-Rotating Vortex Pairs

Previous experimentation by Fabre *et al.* (2002)[3] has determined the greatest growth of instability to occur at $\gamma = 0.37$ in 3 Dimensions.

The average induced fluid velocity at $x = 0$ corresponding to $\gamma = 0.4$ is $v = -1.6404$ for co-rotating pairs (Figure 2.d) and $v = -0.3670$ for counter-rotating pairs (Figure 3.d). This corresponds to $\frac{\Gamma_{\text{effective}}}{\Gamma} = 3.515$ for co-rotating vortices and $\frac{\Gamma_{\text{effective}}}{\Gamma} = 0.7865$ for counter-rotating pairs. This ratio is really measuring the vortex pair magnitude, and not the instability of the pairs. The counter-rotating pairs have a lesser magnitude due to the inner vortices inducing a velocity opposing the downwash produced by the stronger outer vortices.

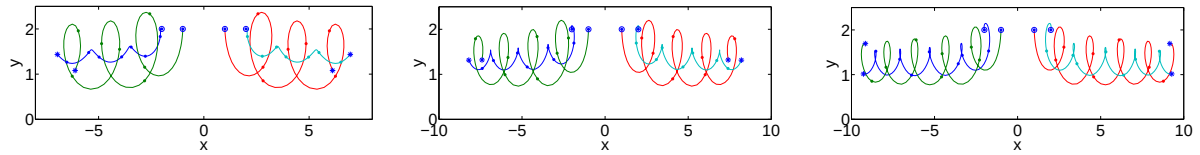

(a) $\gamma = 0.2 \quad t = 15$ s (b) $\gamma = 0.4 \quad t = 15$ s (c) $\gamma = 0.6 \quad t = 15$ s

Figure 4: Symmetric Co-Rotating Vortex Pairs Interacting with Ground, $y = 0$

As the two pairs of co-rotating vortices approach the ground, $y = 0$, they are observed to separate and move in opposing directions. This movement is attributed to the preservation of the impermeability boundary condition. As with free falling co-rotating vortices, the pairs are observed to separate and move apart faster for increasing values of γ.

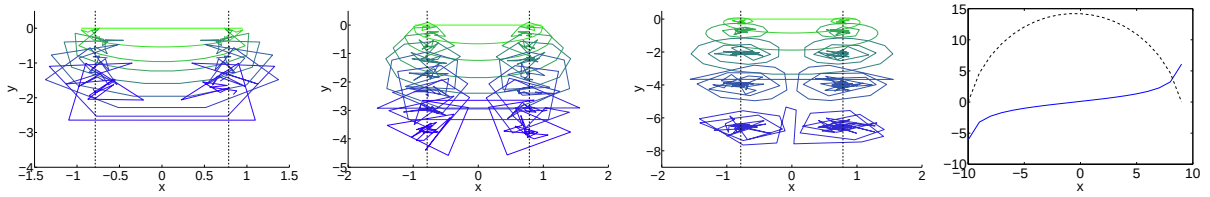

(a) $N = 10 \quad t = 1$ s (b) $N = 20 \quad t = 1$ s (c) $N = 50 \quad t = 1$ s (d) Elliptical Load (black) and Γ Distribution (blue)

Figure 5: Ideal Elliptical Loading with Constituent Vortices

It was shown that as for an ideal elliptically loaded wing (Figure 5.d) of length b modeled as a distribution of vortices, the separation of the constituent two vortices is $\frac{\pi}{4}b$. This slight inward movement of the two "vortices" of vortices is due to the high induced velocity and, therefore, vortex velocity, near $x = 0$ due to the increasing vortex strength away from $x = 0$ seen as the solid line in Figure 5.d.

[1] Increased error enters the simulation as the vortices approach $y = 0$ due to the inviscid approximation and ground effects.

[2] It actually turns out to only be the case for small time spans, since opposing vortex pairs disrupt the steady downward motion.

[3] Fabre, D., Jacquin, L & Loof, A. 2002 Optimal perturbations in a four-vortex aircraft wake in counter-rotating configuration. *J. Fluid Mech.* **451,** 319-328.